Journal of
Nanoscience and Nanotechnology
Vol. 9, 6760–6766, 2009

Fluorescence Correlation Spectroscopy to Study Diffusion Through Diatom Nanopores

Hemant Bhatta[1,*], Jörg Enderlein[2], and Gary Rosengarten[1]

[1] *School of Mechanical Engineering, The University of New South Wales, Sydney 2052, Australia*
[2] *III. Institute of Physics, Georg August University, D-37077 Göttingen, Germany*

The intricate pore architecture of diatom frustules has been extensively studied mainly as the basis of diatom classification. There have, however, been very few reports on understanding the effect of the pore architecture on the movement of molecules through the pores. Information on molecular transport though diatom membrane pores has the potential to help develop more efficient membrane filtration systems. In this paper the transport of molecules through individual diatom nanopores is investigated. Fluorescence correlation spectroscopy (FCS) is used to determine diffusion coefficients. Thus, for the very first time, we measure the effect of the three dimensional pore structure of the diatom *Coscinodiscus wailesii*, on the mean diffusion coefficient through the pores. The results show almost a 50% decrease in the diffusion coefficient relative to that in the free solution.

Keywords: Frustules, Boundary Conditions, Diffusion, Fluorescence, FCS.

1. INTRODUCTION

Diatoms are microscopic, unicellular algae abundantly found all around the world, particularly in moist or submerged surfaces and open water.[1] Both seawater and freshwater are suitable habitats to the numerous diatom species. Diatom colonies in water have been utilized for various applications such as indicators of hydrologic, climatic, environmental and water level changes; indicators of surface water acidity, and also in archaeology, oil and gas exploration, and even in forensic science.[2] Diatoms offer a model biological micro/nanoporous membrane as they dominate aquatic environments that contain a vast array of harmful particles and molecules that are mixed with their nutrients. They thus require an energy efficient filtering process that selectively allows useful molecules to pass through their membrane. As yet, although there are various theories associated with the reason for the intricate nanostructure of their membrane, there is little information on their filtering process. This information is critical for diatom evolutionary biology, and also for using nature to help design more efficient membranes.

Diatoms have been particularly interesting to researchers because of their outer shell structure known as frustules.[3] The frustules are composed of amorphous silica, naturally nano-fabricated, displaying unparalleled diversity in structure and morphology. The unique frustule morphologies have been used by taxonomists to classify the diatoms in an estimated 10,000 different species.[1] The nanoporous structures of the frustules also offer the potential to be used for specialized filtration procedures.[4] These frustule structures with nanometer scale pore diameters can be used for particle filtration and microfiltration,[5,6] in addition, select species with intricate porous structure make the frustule structures suitable as nanofiltration (NF) membranes.[4,7] Thus, in order to understand the filtration functionality of the diatoms, it is necessary to understand the basic diffusion behaviour of molecules through the diatom pores. Ploug et al.[8,9] have conducted diffusivity studies within and around diatoms, however these have been mainly conducted in diatom aggregates rather than individual diatom frustules. Hale and Mitchell studied the particle flow along the surface of diatom frustules but not through the pores.[10] Thus, to the best of our knowledge, there have been no reports on the diffusion study of particles through individual diatom pores. In this study, we look at the random Brownian motion of molecules whilst in and through the pore and thus the effect this has on the actual distance travelled by the molecule. The influence of pore walls on the diffusing species have been illustrated by diffusion studies performed on gels, crowded environments and porous membranes. The hindered diffusion of solutes in gels has been well researched.[11] Lawrence et al. for instance reported reduced diffusion in biofilm proving that in general diffusion coefficients for various molecules through

*Author to whom correspondence should be addressed.

 1533-4880/2009/9/6760/007 doi:10.1166/jnn.2009.2020

biofilms and bioflocs are 50% to 80% of their respective values in water.[12]

Among various methods used to measure diffusion coefficient, fluorescence correlation spectroscopy (FCS) is one of the techniques that has gained considerable popularity in measuring the diffusivity in smaller volumes than conventional fluorescent techniques. FCS can be used to study molecular motion and interaction in solutions that allows for an extremely sensitive determination of molecular diffusion properties, down to the level of single molecules.[13] In FCS, fluorescence fluctuations are detected in a small volume of around 1 fl or less and then autocorrelated yielding an autocorrelation function (ACF) of the fluctuating signal. Where the detection volume consists of a relatively small number of fluorescent molecules, the fluctuations are dominated by the random diffusion of the fluorescent molecules out of that volume and the ACF shows a prominent decay which is characterized by the diffusion coefficient of the molecules. The deduction of diffusion parameters is dependent on the shape of the confocal detection volume. In the standard case of an assumed prolate ellipsoidal Gaussian observation volume, the autocorrelation function is mathematically given as:[14]

$$G_D(\tau) = \frac{1}{N(1+\tau/\tau_D)\sqrt{1+\tau/(\omega^2\tau_D)}} \quad (1)$$

τ_D is the characteristic diffusion time during which a molecule resides in the observation volume, ω is the ratio of the height of the observation volume (z_0) to the width (r_0) i.e., z_0/r_0 and N is the mean number of fluorescent molecules in the observation volume. Further, the more commonly used parameter, diffusivity or the diffusion coefficient (D) is inversely proportional to the diffusion time (τ_D) as given by Eq. (2):

$$\tau_d = r_0^2/4D \quad (2)$$

Equation (1) gives a rather empirical fitting curve which still, however, allows us to extract a mean diffusion time τ from the measured curves. As a demonstration of the use of this equation under similar situations we would like to point to the research work by Iris von der Hocht and Jörg Enderlein[15] where the authors have shown how Eq. (1) can be used to extract diffusion times. They have demonstrated the uncertainty is low using Eq. (1) in pores even though it is derived for a free solution and a 3d-Gaussian detection volume (which in any real experiment is never the case). However all FCS experiments use this equation whether it is applied to a free solution or not, because of the fact that it leads to an analytic expression for the autocorrelation curve. It also fits real data well because it has two rather elastic fit parameters, namely the values of the half axes of the quasi Gaussian distribution. Thus we have used Eq. (1) as a generic fit function for deducing diffusion time, a widely used term that defines molecular mobility. Since, the parameters of the confocal observation volume in FCS match quite well with the pore dimensions of the diatom species, particularly the *Coscinodiscus species* studied here, this technique is well suited for the diffusion studies through diatoms. Since *Coscinodiscus sp.* is one of the widely studied and largest genera of marine planktonic diatoms with diameters up to a few hundreds of micrometers, which has also been investigated for nano-patterning,[16] we chose this species for our study. As described in the paper below, we notice that the organic component of the diatom frustules,[17,18] exhibit autofluorescence and thus require filtering of the final FCS data. This is achieved by using the recently established technique known as Fluorescence Lifetime Correlation Spectroscopy (FLCS). Böhmer et al. introduced the idea in 2001,[19] and since then there have been numerous publications presenting exciting new applications of this method.[20–22] FLCS is used for separating different FCS contributions by using picosecond time-resolved detection system. The separation principal of FLCS is based on time-correlated single photon counting (TCSPC) decay behavior. In FLCS, a separate autocorrelation function is calculated for each fluorescence lifetime component, emitted, for instance, by various species in the sample rather than fitting of a multiple-parameter model to a complex autocorrelation function.[23] Thus, FCS and FLCS have been introduced as tools to understand the molecular mobility within the diatom pore.

2. EXPERIMENTAL METHODS

The diatoms, *Coscinodiscus wailesii* (CCMP2513), were obtained from Provasoli-Guillard National Center for Culture of Marine Phytoplankton, USA. The organic parts were cleaned using sulfuric acid (90%) and hydrogen peroxide (30%) solutions. 5 mL of the diatom solution was mixed with the same amount of sulfuric acid and left under fumehood for about 2 hours at a temperature of around 70 °C. The mixture was then centrifuged at 3000 rpm for 5 mins. The supernatant was removed and the pallet of diatoms was resuspended in distilled water. The centrifugation and washing was repeated for at least five times to remove excess acid. After the last wash, the solution was mixed with equal volume of hydrogen peroxide and placed in a water bath at approximately 70 °C, for about an hour. After cooling, the samples were poured into test tubes and centrifuged at 3000 rpm for 5 minutes. Centrifugation and washing was repeated for at least 5 times with addition of distilled water. The pellet from the final wash, which contained clean diatom frustules were suspended in ethanol.

FCS measurements were conducted with a MicroTime200 inverse time-resolved fluorescence microscope (MT200, PicoQuant, Berlin, Germany). Clean diatoms were placed on a 0.17 mm (#1.5) coverslip. The

diatom frustules were suspended in Oregon Green® 488 (2′,7′difluorofluorescein, Invitrogen, Cat # D6145) dye solution at 250 pico molar concentration which was excited at 470 nm wavelength by pulsed laser diode ((LDH-P-470, PicoQuant, Berlin, Germany)) with repetition rate of 40 MHz. The molecular weight of Oregon Green dye is 368.29, similar to the popular dyes such as Fluorescein or Rhodamine, however, one of the important properties of this dye is that it is extremely photostable and thus resists photobleaching, which is important for FCS measurements, particularly at very low concentration. The laser diode was operated at low laser power of 10 μW. The objective used was 60× water immersion objective from Olympus (UPLAPO 60× W, 1.2 N.A., Olympus Europa, Hamburg, Germany). One of the crucial experimental parameters when working with water immersion objectives is correct adjustment of the objective's correction collar to the actual thickness of the used coverslide. Even small deviations between adjusted and actual thickness can have profound effects on the resulting molecule detection function (MDF).[24] The MDF is important as it determines the shape of the ACF along with the diffusion coefficient of the molecules. The method proposed by Schwertner et al. was used for setting the objective's adjustment collar correctly.[25] Fluorescence was collected by the same objective, passed through filters blocking any laser backscatter, and subsequently focused onto a confocal aperture of 200 μm diameter. The fluorescence signals were detected by single-photon avalanche diodes (SPAD, PDM series, detector diameter 50 μm, Micro Photon Devices, Bolzano, Italy). A dedicated single photon counting electronics (PicoHarp 300, PicoQuant, Berlin, Germany) was used for recording photon detection events in time tagged time-resolved (TTTR) mode with a temporal resolution of 4 ps.[19] The TTTR mode allows for subsequent calculation of fluorescence decay curves (as in time-correlated single-photon counting or TCSPC) and fluorescence correlation curves. FCS measurements were first taken with the clean frustules suspended in a drop of deionized water (100 μL) on the coverslip. 100 μL of the fluorescent dye was then added, allowed to mix with the water solution for about two minutes and then further FCS measurements were taken. The points of interest for FCS measurements were chosen on the transmission image of the diatom frustule. In order to determine the data variability, the measurements for each curve were taken at six different points and in each pore at least three different data points were chosen. The FCS data at each point was collected for a time period of 5 mins and the calculated correlation functions were fitted using the standard Gaussian model.

3. RESULTS

A brief overview of the pore architecture and the three dimensional structure of the diatom frustule is given here. After harsh cleaning with acid and peroxide, most of the diatoms have both the inner and the outer layer intact, whereas in some the outer layer is sometimes washed away leaving only the inner layer with bigger pores. Figure 1 shows the pore architecture of the diatom under study. In Figure 1(a) the outer layer with smaller pores can be seen whereas Figure 1(b) reveals the inner layer with bigger sized holes of diameter 1.2 ± 0.2 μm. By image analysis or alternately by measuring the size of holes in a particular area, the porosity of the inner layer i.e., the ratio of the hole-area to the total-area, can be calculated, which for this layer was $29.0 \pm 2\%$. The layer with the smaller pores has an average pores size of approximately 270 nm and porosity of 14%. The space between these two porous layers forms chambers known as areolae as shown in Figure 1(c). Figure 1(c) is a close up of the frustules sitting at an angle and thus revealing the depth perception and the three dimensional architecture. A schematic is drawn in Figure 1(d) that shows a cross-section view at the dotted line in Figure 1(c). The three dimensional structure of the *Coscinodiscus species* has been thoroughly described in our previous publication,[7] which shows that the thickness of the integrated layer is 1–1.2 μm. Our research interest is quantifying the movement of molecules whilst in the areolae surrounded by the two porous layers.

FCS was used to observe the fluorescence fluctuation of dye molecules passing through the diatom nanopores. The intensities of the fluorescence fluctuation were then correlated in order to deduce the diffusion terms. FCS data were collected for the dye in six different pores of two different diatoms. For comparison, the FCS data were also collected for the dye in free solution. In order to ensure direct comparison of data under exact similar conditions, the free dye solution chosen was in the same sample with the diatoms suspended. For the fluorescence signal in the free dye solution, it was noted that there was no photobleaching of the dye under 10 μW of laser power for the duration of the data acquisition. The cleaned diatom frustules showed some autofluorescence, as shown in Figure 2, which could be contributed to organic compounds, mainly (glyco) proteins, which constitute about 3% of the diatom cell wall.[17, 18] The other 97% of the diatom cell wall consists of inorganic compounds, in particular almost pure hydrated silica doped with trace amounts of aluminum and iron.[26]

The autofluorescence of the diatom bio-silica spreads over a wide emission range, displaying high intensity from 510 nm to 720 nm for 470 nm excitation. In the fluorescence image, we notice that the fluorescence is higher in the solid silica part compared to that in the pore. Direct comparison of the fluorescence image with the SEM images (Fig. 1) illustrates that the hole region seen here (inside the hexagonal structure) actually is the outer layer containing structures of silica forming smaller pores of around 300 nm diameter. Thus, the fluorescence contribution is due to silica and the pores, averaged out here to

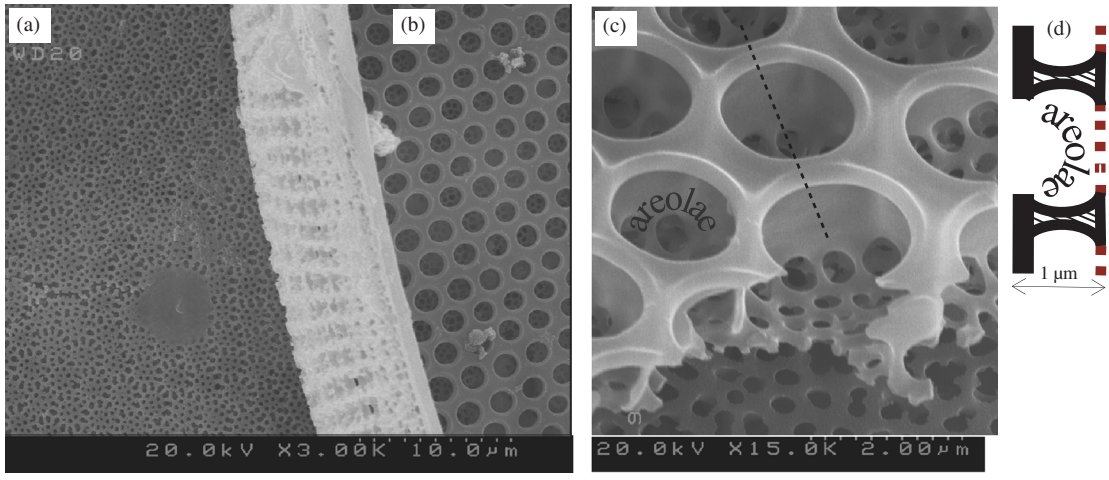

Fig. 1. SEM images showing the pore architecture of *Coscinodiscus wailesii*. (a) The intact outer layer, (b) inner layer only as outer layer is washed away, (c) view from inside showing the inner and outer layer, the dotted line shows the cross sectional region for 'd' and (d) schematic of cross sectional view showing the two-layer pore architecture.

show lower intensity holes as resolving these nanopores is beyond the sensitivity of fluorescence microscopy. In addition, the water solution in the nanopores would contain the fluorescent organic compounds of the diatom frustule that have been dissolved in the water suspension. In live diatoms, the siliceous parts of the diatom are covered by a protective layer, a coating of organic matter (proteins and carbohydrates) that avoids dissolution in the aqueous environment.[27] However, during acid washing this layer has been removed to expose the bio-silica and the components of the washed diatoms dissolve into the solution, albeit a very slow rate.

For FCS experiments, the autofluorescence of diatom frustules acts as unwanted background noise. Thus, before taking the FCS data, the diatom samples were photobleached for few minutes until the autofluorescence signal was minimal and stabilized. The autofluorescence of the diatom frustules affects the FCS data in two ways. Firstly, the autofluorescence adds to the overall photon counts at the sample considerably reducing the signal to noise ratio, and thus making the autocorrelation curve difficult to analyse for diffusion deductions. Secondly, the organic compounds that get dissolved in the solution would exhibit their own fluorescence and thus affect the final autocorrelation curves. Hence, during the experiment, the autofluorescence was suppressed as much as possible by the photobleaching and in addition the autofluorescence signals, without the addition of dye, were recorded to create a filter for correcting the final data. FCS fits for the diffusion of dye in the diatom pores were thus obtained by curve fitting of the filtered fluorescence data.

Normalized TCSPC histograms at the diatom pore for the autofluorescence and with the addition of the dye are shown in Figure 3. Here Y-axis represents the photon counts and X-axis represents the delay time or channel number. The channel number is a representation of the delay time measured relative to the excitation pulses and contains information about the fluorescence decay on a nanosecond timescale.[23] In TCSPC, this time scale is

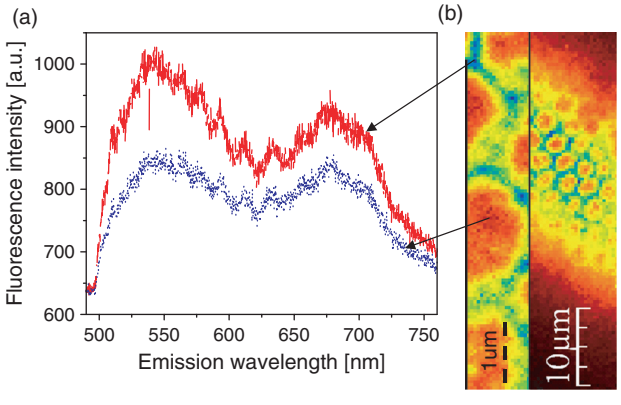

Fig. 2. (a) Autofluorescence spectra of diatom frustule excited with 470 nm light at the silica (solid line) and the pore (dotted line). (b) Confocal fluorescence microscopy image showing the autofluorescence exhibited by the diatom frustules.

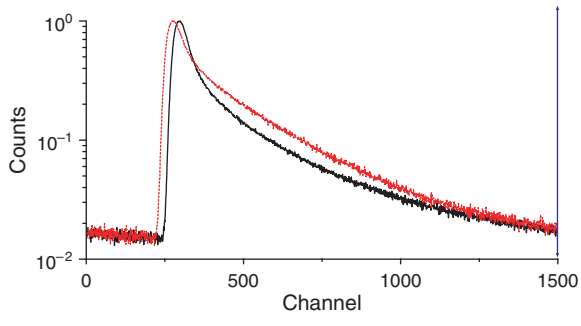

Fig. 3. Normalized TCSPC histograms measured at the pore before adding the dye i.e., autofluorescence (solid line) and after adding the dye (dashed line).

binned into N channels, typically on the order of 100–1000. The solid line represents the decay pattern for the autofluorescence and the dashed line is superposition of the contribution from the dye and the autofluorescence signal. FLCS is then used to extract the contribution of the dye alone at the diatom pore by filtering out the autofluorescence signal.

Figure 4(a) shows the unfiltered autocorrelation curve at the diatom pore. The autocorrelation curve of Figure 4(b) represents the data in the pore when there was no dye added. Thus, this represents the signal due to the autofluorescence of the organic compounds of the diatom bio-silica. This signal is used as a filter component. The filtration procedure was based upon the FLCS technique, which was performed using custom made add-ons to the data analysis software OriginPro7 from OriginLab.

The final filtered data for the diffusion of dye in the diatom pore is shown in Figure 5. The graph shows the autocorrelation curves and the numerical fits obtained for the free dye diffusion and the dye diffusing in the diatom pore. Here, we notice that the filtering yielded good quality fit as judged from the fit residuals in Panel (A) of Figure 5. The diffusion times can be deduced from the correlation

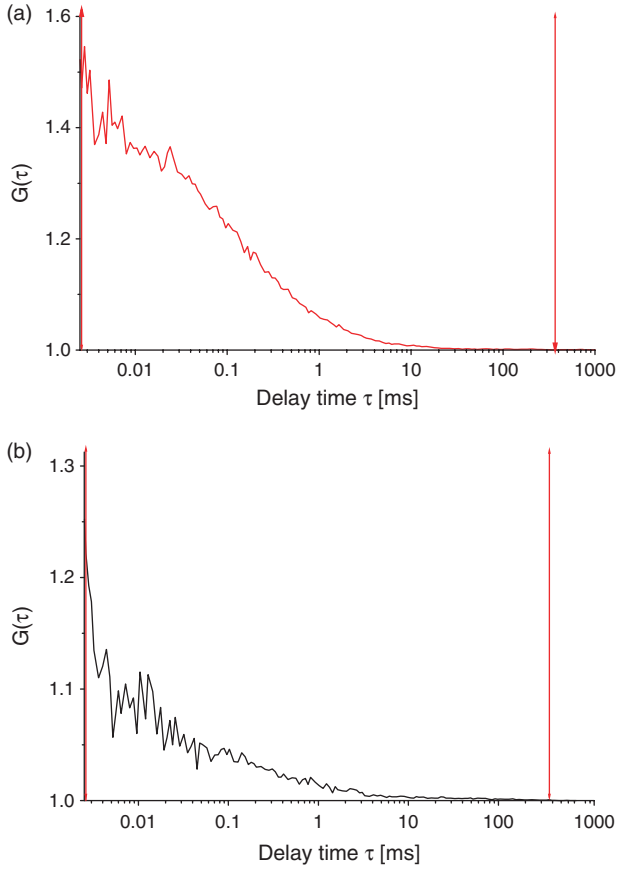

Fig. 4. (a) Autocorrelation curve for the fluorescence of the dye at the diatom pore. (b) Autocorrelation curve obtained from autofluorescence of the diatom bio-silica (no dye added).

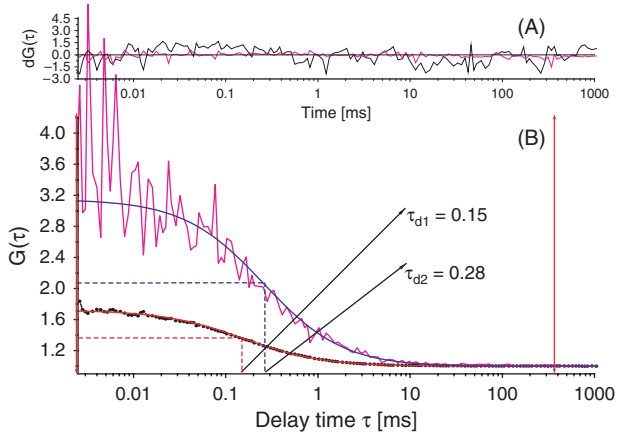

Fig. 5. Panel (B)—FCS autocorrelation curves and fits for the diffusion of dye in free solution (bottom curve, (B)) and in the diatom pore (top curve, (B)). The dotted lines show the diffusion times, i.e., the delay time at half maximum. Panel (A)—residuals of the fits showing good fit of experimental data to the Gaussian model.

curves by taking the delay time at half maximum. Thus, the diffusion time for the dye in free solution was observed to be 0.15 ± 0.02 ms. Müller et al.[28] have reported an absolute diffusion coefficient of 4.11×10^{-10} m^2/s for Oregon Green dye whose molecular size is 5.95 Å. This corresponds to a diffusion time of 0.17 ms for the dye in the free solution which is similar to the value that we have obtained. As part of control measure we used a region of interest in the solution just outside of the diatom frustule. The FCS results for those measurements corresponded well with the diffusion value of the free dye with diffusion time of 0.15 ms. It should be noted that the diffusion results obtained by Müller et al. are presented here merely as reference and to show that our experiments results are comparable. The diffusion values would vary depending on the optical setup and experimental conditions used. It is hard to obtain absolute diffusion coefficients by FCS technique as there are various limiting factors associated with its sensitivity as discussed thoroughly by Enderlein et al. where the authors introduce two-focus FCS setup in order to determine the absolute diffusion values.[29] We are more interested in the difference between diffusion properties in the free solution and in the pore rather than the absolute values. All our data are however taken under same experimental setups thus there should be no effect in direct comparison between results. The diffusion time for the dye in the pore is 0.28 ± 0.01 ms which is higher as compared to the diffusion time in the free solution. Since diffusion time is inversely proportional to the diffusion coefficient (Eq. (2)), it is observed that the diffusivity in the diatom pore is lower than in the free solution. The diffusion parameters are dependent on the shape and size of the observation volume; however, here we have compared the data in the diatom pore to the diffusion data in free solution taken under similar experimental setup.

4. DISCUSSION

The random Brownian motion of molecules in and through the intricate three dimensional structure of the diatom is the diffusion phenomenon that is of interest. Here, we discuss the change in diffusion time or diffusivity of the fluorescent dyes passing through diatom nanopores by using FCS. As shown by the SEM images, the diatoms have intricate three dimensional structures with two layers of pore architecture. One would expect an influence of this unique pore structure on the random motion of molecule through these pores. In order to study and quantify this effect, we looked closely into a single pore by the technique of FCS. As the FCS confocal volume has a waist of around 300 nm and height of around 1 μm, this serves well for studying the diatom nanopore which has diameter (for the smaller pores) of around 300 nm and thickness of around 1 μm.[7] The FCS results showed that the diffusivity in the pore was lower than diffusivity in free solution by a factor of 1.8 i.e., (0.28/0.15). These results imply that the random motion of the dye molecules is decreased by nearly half due to the pore geometry. Here, it is important to mention that the observation is certainly not a simple geometric restriction effect since pure geometrical confinement will mostly lead to an apparent *increase* of the diffusion coefficient (due to restriction and thus decrease of the effective detection volume), as can be seen in Figures 3(A–C) in the paper by Hocht and Enderlein.[15] However, in our research within diatom nanopores, we notice a *significant decrease* of the diffusivity (i.e., increase of diffusion time). Possible explanation to the increased diffusion time could be that the pore geometry is such that at the entrance/exit of the pore, a dye molecule faces the edge of the pore and possibly some entropic force fields. Dinsmore et al. indicate that passive structures etched into the walls of a container create localized entropic force fields which can trap, repel or induce the controlled drift of particles.[30] The authors have further shown that a pronounced free energy barrier exists when particles are at the edge of a structure, thus pushing the particle back away from the edge (observations made perpendicular to the edge). The motion of particles along the direction parallel to the edge exhibited free diffusion. One of the reasons that the dye molecule remains in the observation volume for a longer time could be contributed to the free energy barrier that essentially reflects the molecule back into the pore volume. Thus, the pore geometry enforces a freely moving dye molecule to remain in the pore longer than it would in a free solution (even though the molecule to pore size ratio is very low i.e., <0.01) hence decreasing the diffusion coefficient. The rapid changing pore size with depth that exists in the diatom frustule could be an ideal design for maximising entropic trapping. In an independent experiment conducted using epi-fluorescence microscopy (data not shown) we observed a reduction in the diffusivity of dye molecules and deduced a similar value of approximately 1.8 for 'tortuosity.' Tortuosity, in essence, defines the tortuous path a diffusing molecule has to take. Higher values of tortuosity will thus decrease the average diffusion coefficient through the pores.[31] Thus, molecules traverse in random tortuous path whilst travelling through the double layer nanostructure of the diatom frustule and hence take longer time to exit the diatom pore. Hence, we conclude that the mobility of molecules inside a diatom pore is affected by the pore geometry of the diatom structure, thus slowing the random walk of a molecule by a factor of nearly two. In order to check for any spatial variability in the sample we checked diffusion values at various random locations within the nanostructure. As they are all identical within the experimental error, we have inferred that there is little or no spatial variability. Also, spatial variability would be rather difficult to analyze as the standard objective used during FCS measurements is 60× which does not give enough magnification and resolution to localize points within nanostructure with good repeatability.

5. CONCLUSIONS

We have studied the basic diffusion properties of molecules through a diatom frustule. The diffusion times have been measured, and it has been found that diffusion rates are greatly influenced by interactions between diffusing species and pore walls. It is well known that the diffusing species experience hindrance whilst passing through gels and porous membranes ultimately reducing the diffusion coefficient by up to 80% of their respective values in free solution. The centric diatom species under investigation *Coscinodiscus wailesii*, which has two layers of porous silica shows a diffusion time of 0.28 ms, a longer time compared to the diffusion in free solution that is 0.15 ms. This increase in diffusions time or decrease in diffusion coefficient by factor of nearly two as compared to the bulk diffusivity can be contributed to the unique architecture of the diatom frustule which is around one micron thick with two layers of nanoporous structures and imposes different boundary conditions to the flow of the particles. Thus the observed increase in diffusion time is the result of confinement effects inside the pore. Our measurements give quantitative estimates of how long molecules are retained in the pore due to the geometric confinement and the peculiarities of pore geometry, which is precisely the prupose of this study. These basic diffusion studies through the diatom frustules have shed some light on the particle flow through the unique cell structure of the frustules. The lower rate of particle diffusion may have an effect on the nature of nutrient intake by these organisms. On the one hand this knowledge helps in understanding of molecular mobility in diatom frustules and on the other this information could be used in utilizing the diatom frustules pore architecture to design membranes.

Acknowledgment: We thank the support of ARC/NHMRC network on Fluorescence Applications in Biotechnology and Life Sciences (FABLS) grant number RN0460002 and the support of CSIRO—Water for a Healthy Country Flagship under Advanced Membrane Technologies for Water Treatment Research Cluster. We are also grateful for the support of Anastasia Loman and Jana Humpoličkova with the FCS system at the University of Tübingen and the useful discussions with Jim Mitchell.

References and Notes

1. G. R. Hasle, The Biology of Diatoms, edited by D. Werner, Blackwell Scientific Publications, Oxford **(1977)**.
2. F. E. Stoermer and P. J. Smol, The Diatoms: Applications for the Environmental and Earth Sciences, Cambridge University Press, Cambridge **(2001)**.
3. F. E. Round, R. M. Crawford, and D. G. Mann, The Diatoms, Cambridge University Press, Cambridge **(1990)**.
4. J. Parkinson and R. Gordon, *Trends Biotechnol.* 17, 190 **(1999)**.
5. P. F. Schuler, M. M. Ghosh, and P. Gopalan, *Water Res.* 25, 8 **(1991)**.
6. E. J. Ongerth and P. E. Hutton, *Journal of American Water Works Association* 89, 12 **(1997)**.
7. D. Losic, G. Rosengarten, J. G. Mitchell, and N. H. Voelcker, *J. Nanosci. Nanotechnol.* 6, 982 **(2006)**.
8. H. Ploug and U. Passow, *Limnology and Oceanography* 52, 1 **(2007)**.
9. H. Ploug, S. Hietanen, and J. Kuparinen, *Limnology and Oceanography* 47, 4 **(2002)**.
10. M. S. Hale and J. G. Mitchell, *Nano Lett.* 2, 6 **(2002)**.
11. N. Fatin-Rouge, K. Starchev, and J. Buffle, *Biophysical Journal* 86, 5 **(2004)**.
12. J. R. Lawrence, G. M. Wolfaardt, and D. R. Korber, *Appl. Environ. Microbiol.* 60, 4 **(1994)**.
13. K. Bacia and P. Schwille, Fluorescence correlation spectroscopy, Lipid Rafts, Humana Press **(2007)**, Vol. 398, pp. 73–84.
14. S. T. Hess, S. Huang, A. A. Heikal, and W. W. Webb, *Biochemistry* 41, 3 **(2002)**.
15. I. von der Hocht and J. Enderlein, *Experimental and Molecular Pathology* 82, 2 **(2007)**.
16. D. Losic, J. G. Mitchell, and N. H. Voelcker, *New J. Chem.* 30, 6 **(2006)**.
17. T. Nakajima and B. E. Volcani, *Science* 164, 3886 **(1969)**.
18. D. M. Swift and A. P. Wheeler, *Journal of Phycology* 28, 2 **(1992)**.
19. M. Böhmer, F. Pampaloni, M. Wahl, H.-J. Rahn, R. Erdmann, and J. Enderlein, *Rev. Sci. Instrum.* 72, 11 **(2001)**.
20. A. Benda, M. Hof, M. Wahl, M. Patting, R. Erdmann, and P. Kapusta, *Rev. Sci. Instrum.* 76, 3 **(2005)**.
21. J. Enderlein and I. Gregor, *Rev. Sci. Instrum.* 76, 3 **(2005)**.
22. M. Böhmer, M. Wahl, H.-J. Rahn, R. Erdmann, and J. Enderlein, *Chem. Phys. Lett.* 353, 5 **(2002)**.
23. P. Kapusta, M. Wahl, A. Benda, M. Hof, and J. Enderlein, *Journal of Fluorescence* 17, 1 **(2007)**.
24. J. Enderlein, I. Gregor, D. Patra, T. Dertinger, and B. Kaupp, *ChemPhysChem* 6, 11 **(2005)**.
25. M. Schwertner, M. J. Booth, and T. Wilson, *Journal of Microscopy* 217, 3 **(2005)**.
26. F. Noll, M. Sumper, and N. Hampp, *Nano Lett.* 2, 2 **(2002)**.
27. H. E. Townley, A. R. Parker, and H. White-Cooper, *Adv. Funct. Mater.* 18, 2 **(2008)**.
28. C. B. Müller, A. Loman, V. Pacheco, F. Koberling, D. Willbold, W. Richtering, and J. Enderlein, *European Physics Letters* 4 **(2008)**.
29. T. Dertinger, V. Pacheco, I. von der Hocht, R. Hartmann, I. Gregor, and J. Enderlein, *ChemPhysChem* 8, 3 **(2007)**.
30. A. D. Dinsmore, A. G. Yodh, and D. J. Pine, *Nature* 383, 6597 **(1996)**.
31. C. N. Satterfield, C. K. Colton, and W. H. J. Pitcher, *AIChE J.* 19, 3 **(1973)**.

Received: 5 December 2008. Accepted: 23 March 2009.